ISSN Online: 2756-3898, ISSN Print: 2714-500X

https://doi.org/10.47514/phyaccess.2025.5.2.002

Plasmonic Enhancement and Lifetime Extension of Perovskite Solar Cells via Biosynthesized Silver Nanoparticles Integration

Jamila Tasi'u^{1,2}, Muhammad Y Onimisi², Eli Danladi³, Kurawa S Mustafa⁴, Haruna Ali², Kehinde Ogunmoye⁵, John C Izang⁶ and Hameed A Lawal⁷

- ¹ Department of Physics, Kaduna State University, Kaduna, Kaduna State, Nigeria
- ² Department of Physics, Nigerian Defence Academy, Kaduna, Kaduna State, Nigeria
- ³ Department of Physics, Federal University of Health Sciences, Otukpo, Benue State, Nigeria
- ⁴ Department of Physics, Sa'adatu Rimi University of Education, Kano, Kano State, Nigeria
- ⁵ Department of Physics and Astronomy, Appalachian State University, Boone, North Carolina, USA
- ⁶ Department of Chemistry, Wayne State University, Detroit, Michigan, USA
- ⁷ Department of Physics, Airforce Institute of Technology, Kaduna, Kaduna State, Nigeria

Corresponding E-mail: jtikbai@gmail.com

Received 05-05-2025 Accepted for publication 16-07-2025 Published 24-07-2025

Abstract

Perovskite solar cells (PSCs) have attracted significant scholarly attention in the field of photovoltaics due to their simple fabrication process and low cost. However, their potential for commercial use is limited by issues such as low power conversion efficiency (PCE) and instability. In this study, an approach for enhancing both the performance and life time cycle of perovskite solar cells (PSCs) by integrating biosynthesized silver nanoparticles (AgNPs) into the device structure was demonstrated. Unlike previous works that mainly focus on chemical synthesis of plasmonic nanoparticles, this method employs an eco-friendly biosynthesis route, offering a sustainable alternative. PSCs fabricated with varying AgNP concentrations (0–250 μL) exhibited significant improvements, with power conversion efficiency (PCE) increasing from 2.65% to 5.35%, and device lifetime extended by 69% relative to the control device. The observed enhancement is attributed to the plasmonic effects of AgNPs, which enhance light absorption, improve charge carrier extraction, and increase conductivity. This work highlights a promising strategy for the development of more durable and efficient PSCs through green nanotechnology.

Keywords: Silver Nanoparticles; perovskite solar cell; degradation; Surface Plasmon.

I. INTRODUCTION

Perovskite solar cells, classified as third-generation solar technologies, are a form of thin-film solar cells that utilize perovskite materials as the active layer for converting sunlight into electricity. They have garnered widespread interest due to their impressive power conversion efficiency (PCE) and the

potential for low-cost, large-scale production [1, 2]. Despite remarkable progress, PSCs face persistent challenges related to device stability and long-term performance degradation, which have limited their viability for commercialization.

The use of noble metal nanoparticles such as silver (Ag), gold (Au), copper (Cu), etc., has created a pathway to mitigate this limitation. These metallic nanoparticles have gained

interest for their localized surface plasmon resonance (LSPR) properties, which enhance light absorption, exciton generation, and charge transport within photovoltaic devices [3]. Several studies have demonstrated the performance improvements enabled by AgNPs across a variety of solar technologies, including organic [4, 5, 6], silicon-based [7, 8], and dye-sensitized solar cells [9]. However, direct incorporation of metallic nanoparticles into the perovskite layer often leads to stability issues, including enhanced recombination and degradation due to back electromotive force (EMF) reactions [10, 11]. To mitigate these effects, insulating shells such as TiO₂ or SiO₂ have been employed, but these can also hinder charge transport [12, 13].

To address these limitations, we propose the integration of biosynthesized AgNPs stabilized with soluble starch into the PSC architecture. The biosynthesis approach offers multiple advantages, including the use of soluble starch as both a reducing and capping agent, which forms a natural insulating layer that prevents direct metal-perovskite contact, enhances stability, and maintains efficient charge transport. Furthermore, this green synthesis route contributes to environmentally friendly manufacturing processes, aligning with the global push for sustainable renewable energy technologies.

In this study, we fabricated PSCs incorporating varying concentrations of biosynthesized AgNPs (0–250 $\mu L)$ and systematically investigated their performance and degradation behavior. Devices fabricated in ambient conditions demonstrated notable improvements in both PCE and operational lifetime, with enhancements of approximately 19% and 69%, respectively, compared to the AgNP-free device. These gains are primarily attributed to improved light trapping, reduced recombination losses, and enhanced carrier transport facilitated by the plasmonic AgNPs.

This work highlights a sustainable strategy for enhancing both the performance and durability of PSCs through green nanotechnology.

II. METHODS

A. The Perovskite Absorber (CH₃NH₃PbI₃)

The perovskite absorber was prepared by mixing methylammonium iodide (MAI) (0.198 g) and lead iodide (PbI₂) (0.579 g) in γ -butyrolactone (GBL) (650 μ L) and dimethyl sulfoxide (DMSO) (350 μ L) at 70°C for 11 hours.

B. Preparation of Copper(I) Thiocyanate (CuSCN)

Copper(I) thiocyanate (CuSCN) mesoporous layers were prepared using a modified sol-gel method. Copper (I) thiocyanate powder was diluted in dipropyl (10 mg/mL) to obtain the required concentration.

C. Preparation of the Photoanodes

The fabrication of the solar cells involved a series of deposition steps, beginning with cleaning the FTO glass substrates using cotton wool and ethanol. A compact TiO₂ (c-

TiO₂) blocking layer was then screen-printed onto the cleaned glass substrates using a 90-mesh screen to enhance adhesion. This layer was dried at 200°C for 5 minutes and subsequently annealed at 500 °C for 60 minutes to improve interfacial contact. Next, a mesoporous TiO₂ (m-TiO₂) layer was spin-coated onto the substrate at 1000 rpm, dried at 120 °C for 5 minutes, and annealed at 450 °C for 30 minutes.

For the reference cell (Device A), a perovskite absorber layer was spin-coated onto the mesoporous TiO₂ and annealed at 100 °C for 30 minutes. The hole-transporting material, Copper (I) Thiocyanate (CuSCN), was then spin-coated at 1000 rpm, increased to 4000 rpm for drying, and further dried on a hotplate at 60 °C for 5 minutes. Finally, a 120 nm-thick copper layer was deposited as the back contact under high vacuum (10⁻⁵ mbar) using a shadow mask, completing the cell assembly.

For the other five devices (Devices B, C, D, E, and F), biosynthesized silver nanoparticles (AgNPs) were deposited onto the mesoporous TiO₂ layer by spin-coating, with varying volumes (50, 100, 150, 200, and 250 μL). This was followed by annealing at 150 °C for 5 minutes. The perovskite absorber layer was then spin-coated onto the AgNP-modified TiO₂ layers and annealed at 100°C for 30 minutes. The CuSCN hole-transporting layer was deposited using the same spin-coating and drying steps as for the reference cell. Finally, a 120 nm-thick copper layer was deposited as the back contact under high vacuum, using a shadow mask to complete the cell assembly.

D. Solar Cell Assembly

The six photoanodes and counter electrodes were sealed with ethylene-vinyl acetate (EVA) to form the six Perovskite Solar Cells. A schematic diagram of the six solar cells with varying concentrations of bio-synthesized AgNPs and the metal back contact is shown in Fig. 1.

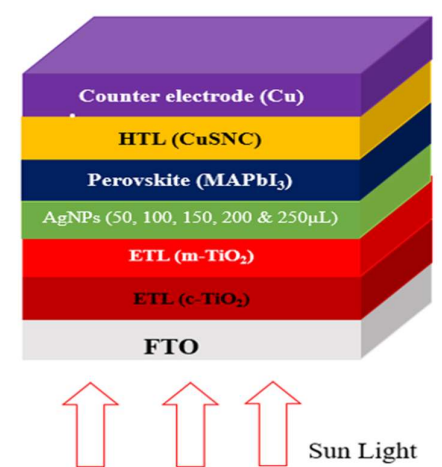


Fig. 1. Schematic diagram of the fabricated PSCs device.

E. Device and film measurement

The current-voltage performance of the PSCs are estimated under AM 1.5G irradiation using a setup involving a Xenon

lamp, an AM 1.5 light channel, and an Electrochemical Analyzer (Keithley 2400 source meter). The efficiency of all the devices was calculated using (1) and (2).

$$FF = \frac{J_{max} \times V_{max}}{J_{max}} \tag{1}$$

$$FF = \frac{f_{MAC} \times f_{MAC}}{J_{SC} \times V_{OC}}$$

$$\eta = \frac{FF \times J_{SC} \times V_{OC}}{P_{IRRADIANCE}} \times 100\%$$
(2)

Where FF is Fill Factor, η is solar cell efficiency, V_{max} is maximum voltage, J_{max} is maximum current density, J_{sc} is short circuit current density, V_{oc} is open circuit voltage and $P_{IRRADIANCE}$ is light intensity.

III. RESULTS AND DISCUSSION

A. Current Density-Voltage (J–V) Measurements

Current density-voltage (J-V) measurements were

performed on the fabricated PSCs under both illuminated and dark conditions, with additional measurements taken after 30 days of storage under ambient conditions. The unmodified device is labeled as sample A, while the devices incorporating various concentrations of biosynthesized silver nanoparticles (AgNPs) are labeled as Samples B to F. The key photovoltaic parameters, short-circuit current density (Jsc), open-circuit voltage (Voc), fill factor (FF), and power conversion efficiency (PCE), were extracted from the J-V curves and are presented in Fig. 2 and 3.

The J-V measurements revealed that the inclusion of AgNPs in the TiO2 photoanode significantly improved device performance, particularly at concentrations of 50 and 100 µL. Compared to the unmodified device (sample A), Sample B (50 μL AgNPs) exhibited notable improvements.

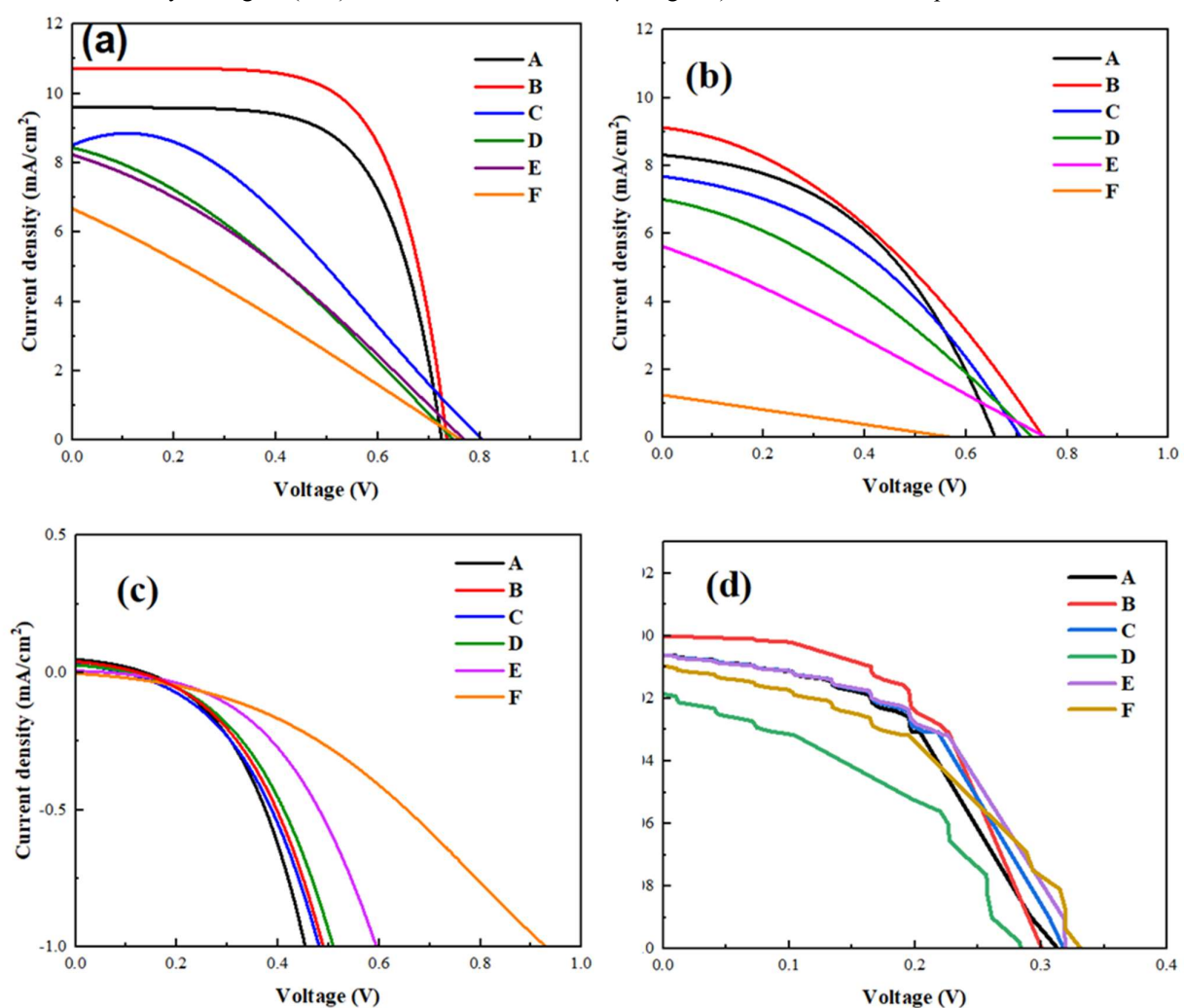


Fig. 2. J-V curves of devices A, B, C, D, E, and F measured under (a) illumination (first measurement), (b) illumination (second measurement), (c) dark conditions (first measurement), and (d) dark conditions (second measurement after one month).

showed an increase in short-circuit current density (J_{sc}) from circuit voltage (Voc) from 0.72 to 0.75 V, and power

In the first scan, the device with 50 μL AgNPs (Sample B) 9.49 to 10.21 mA/cm², fill factor (FF) from 0.61 to 0.77, open-

conversion efficiency (PCE) from 4.49 to 5.35%. After 30 days, the second scan revealed Jsc increased from 8.34 to 9.11 mA/cm², FF from 0.41 to 0.54, Voc from 0.66 to 0.71 V, and PCE from 2.66 to 4.52%, representing a 19.15% improvement in PCE and a 69.92% enhancement in device longevity compared to the reference PSC. For the device with 100 μL AgNPs (Sample C), the first and second scans showed Jsc values of 8.37 and 7.72 mA/cm², Voc values of 0.77 and 0.74 V, FF values of 0.48 and 0.43, and PCE values of 3.09 and 2.33%, respectively. At higher AgNP concentrations (150–250 μL), performance declined, with Sample D (150 μL) showing PCEs of 2.04 and 1.84%, Sample E (200 μL) displaying PCEs of 2.04 and 1.84%, and Sample F (250 μL) dropping significantly to 1.43 and 0.19% for the first and second scans, respectively.

This performance degradation at higher AgNP concentrations is attributed to nanoparticle aggregation, which increases electron-hole recombination sites and reduces catalytic activity. The observed enhancement in device

performance at optimal AgNP concentrations is primarily attributed to improved electron extraction and reduced recombination losses at the TiO₂/Ag interface [16], enhanced light scattering and photon trapping facilitated by AgNP-induced surface plasmon resonance (SPR) effects [17], increased photoactive behavior enhancing exciton generation and charge separation at the TiO₂/perovskite interface [11].

Furthermore, silver, known for its catalytic activity [18], promotes charge transfer kinetics when supported on metal oxide substrates such as TiO₂ [11]. However, excessive AgNPs lead to clustering, counteracting these benefits and creating recombination centers, thus decreasing overall device efficiency [19, 20]. Fig. 2 and 3 clearly illustrate the trend in Voc, Jsc, FF, and PCE with varying AgNP concentrations. The photovoltaic parameters of the devices are summarized in Table I. The data show that a moderate concentration of AgNPs (50 μL) yields the highest PCE and best device stability over 30 days.

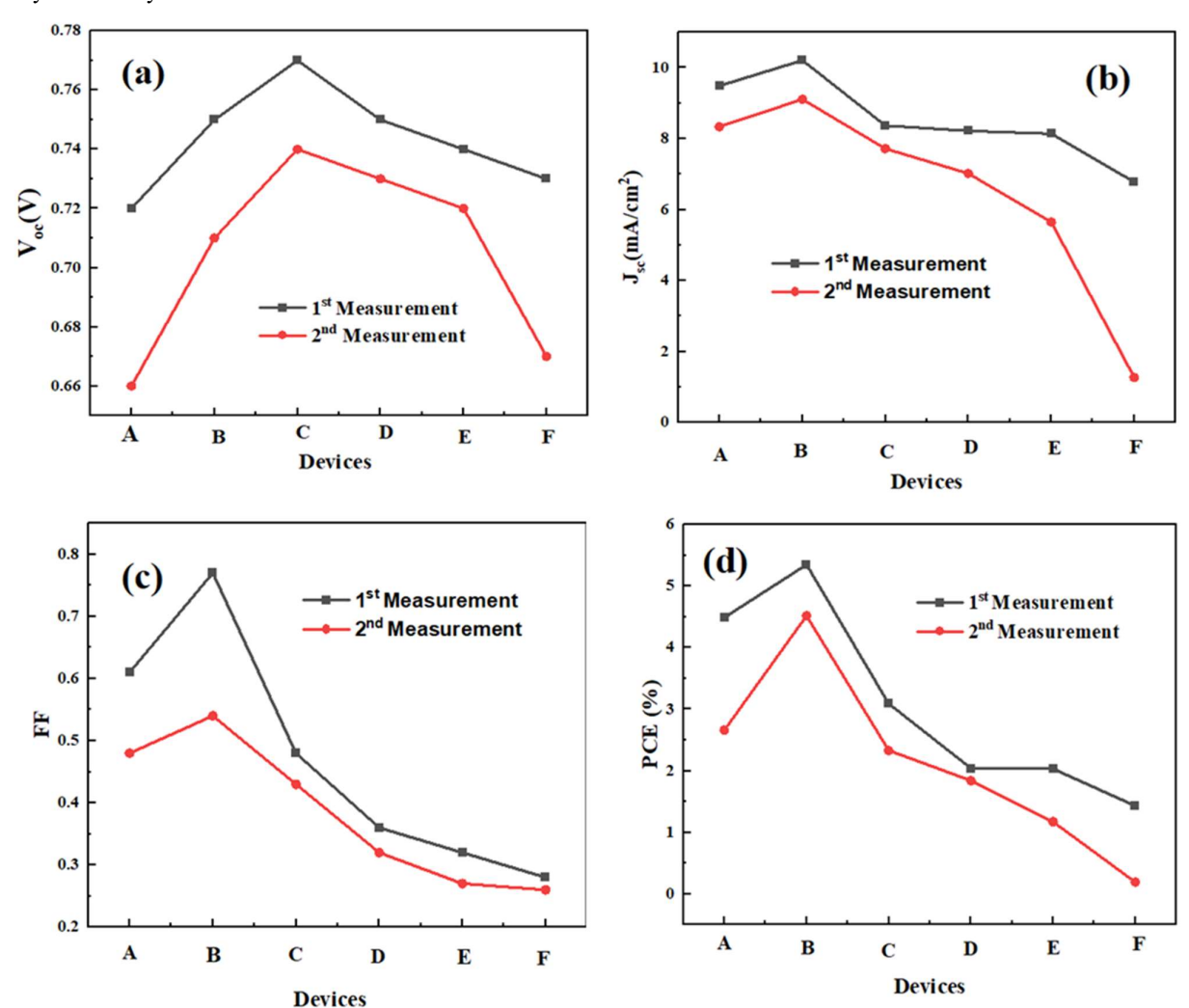


Fig. 3. Statistics of device performance parameters (a) Voc, (b) Jsc, (c) FF and (d) PCE of prepared PSC devices.

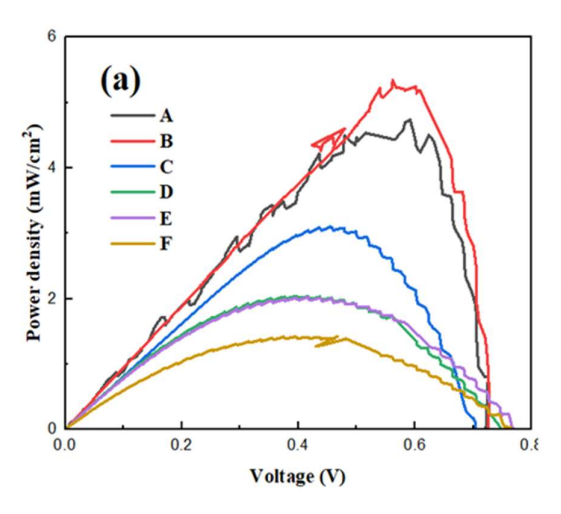
Sample	AgNPs Volume	Jsc	Voc	FF	PCE
	(µL)	(mA/cm ²)	(V)		(%)
A (Reference)	0	9.49 / 8.34	0.72 / 0.66	0.61 / 0.41	4.49 / 2.66
В	50	10.21 / 9.11	0.75 / 0.71	0.77 / 0.54	5.35 / 4.52
C	100	8.37 / 7.72	0.77 / 0.74	0.48 / 0.43	3.09 / 2.33
D	150	8.22 / 7.02	0.75 / 0.73	0.32 / 0.36	2.04 / 1.84
Е	200	8.14 / 5.65	0.74 / 0.72	0.32 / 0.27	2.04 / 1.84
F	250	6.78 / 1.27	0.73 / 0.67	0.28 / 0.26	1.43 / 0.19

Table I. Photovoltaic parameters of PSCs with different AgNP concentrations.

B. Power Density-Voltage Measurements

Fig. 4 displays the power density-voltage (P-V) measurements for both modified and unmodified devices. The maximum power outputs for the devices in the two measurements were as follows: Device A achieved 4.49 and 2.66 mW/cm², Device B attained 5.35 and 4.52 mW/cm².

Device C recorded 3.09 and 2.33 mW/cm². Device D yielded 2.04 and 1.84 mW/cm², Device E obtained 1.03 and 1.17 mW/cm², and Device F produced 1.43 and 0.19 mW/cm². Notably, Device B exhibited approximately a 19% increase in power output compared to the pure TiO₂ device without silver nanoparticles, confirming the positive impact of AgNP incorporation on device performance.



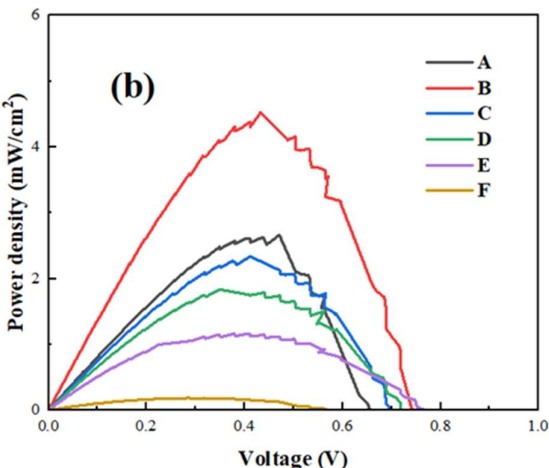


Fig. 4. (a) First measurement P–V curves device A, B, C, D, E and F (b) second measurement P–V curves device A, B, C, D, E and F.

C. Degradation of the Devices

To assess the degradation behavior of the fabricated perovskite solar cells (PSCs), the devices were stored in a desiccator under dark conditions for a period of 30 days after the initial measurement. Subsequent measurements were performed, with the results summarized and illustrated in Table II and Fig. 5, respectively.

The results revealed varying degrees of power conversion efficiency (PCE) degradation among the devices. Devices A and F exhibited the highest degradation rates, with PCE losses of 1.83 and 1.24%, respectively, indicating potential stability challenges. In contrast, Device D showed the lowest degradation, at only 0.20%, suggesting enhanced resistance to degradation factors. Device B, which initially demonstrated the highest PCE (5.35%), also displayed relatively low degradation (0.83%), maintaining its efficiency well over time. Conversely, Device F, which started with a low initial

PCE (1.43%), experienced significant performance loss after ageing.

Table II. Degradation of Power Conversion Efficiency (PCE) after 30 days of storage.

Device	Initial PCE	PCE after 30 Days	Degradation
	(%)	(%)	(%)
A	4.49	2.66	1.83
В	5.35	4.52	0.83
C	3.09	2.33	0.76
D	2.04	1.84	0.20
E	1.03	1.17	0.14
F	1.43	0.19	1.24

Generally, the analysis highlights notable differences in stability across the PSCs, with Device B exhibiting a strong balance between high initial performance and moderate stability, while Device D showed superior long-term stability despite lower initial efficiency.

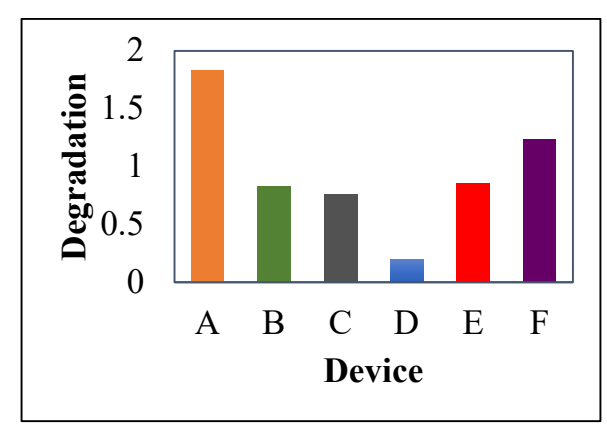


Fig. 5. Degradation level of device A, B, C, D, E and F PSCs.

These findings suggest that both nanoparticle concentration and distribution significantly affect not only device performance but also degradation behavior. Further investigations into material properties, encapsulation strategies, and environmental effects are recommended to better understand and mitigate degradation mechanisms, ultimately enhancing the operational lifetime of PSCs.

IV. CONCLUSION

In this work, a sustainable and effective strategy to enhance both the performance and operational stability of perovskite solar cells (PSCs) through the integration of biosynthesized silver nanoparticles (AgNPs) was demonstrated. Utilizing soluble starch as a green reducing and capping agent, the AgNPs provided significant improvements in light absorption, charge carrier transport, and recombination suppression. Devices incorporating optimized AgNP concentrations exhibited a 19% increase in power conversion efficiency (PCE) and a 69% extension in operational lifetime compared to control devices fabricated without AgNPs.

Beyond performance gains, this study highlights the potential of eco-friendly nanoparticle synthesis routes in addressing the critical stability challenges faced by PSC technologies. The self-capping nature of biosynthesized AgNPs offers a promising alternative to conventional metaloxide encapsulation methods, facilitating efficient charge extraction while minimizing degradation risks.

Future research will focus on fine-tuning nanoparticle size and distribution, as well as integrating biosynthesized plasmonic materials into large-area or flexible PSC devices. This approach could pave the way for more sustainable and commercially viable photovoltaic technologies.

ACKNOWLEDGMENT

The authors gratefully acknowledge the financial support provided by the Tertiary Education Trust Fund (TETFund), Nigeria, through its Academic Staff Training and Development (AST&D) programme, for the sponsorship of the PhD study that culminated in this research work. The

findings and publication of this article would not have been possible without this invaluable support.

References

- [1] A. Kojima, K. Teshima, Y. Shirai and T. Miyasaka, "Organometal halide perovskites as visible-light sensitizers for photovoltaic cells," Journal of the American Chemical Society, vol. 131, pp. 6050– 6051, 2009. https://doi.org/10.1021/ja809598r.
- [2] Z. Qu, F. Ma, Y. Zhao, X. Chu, S. Yu and J. You, "Updated progresses in perovskite solar cells," Chinese Phy. Lett., vol. 38, 107801, 2021. https://doi.org/10.1088/0256-307X/38/10/107801.
- [3] W. Z. Da, Y. Y. Ming, L. L. Ling, L. Ming, J.D. Shi, C.C. Di, C.L. Tung and D.Q. Yan, "Enhanced efficiency and stability of planar perovskite solar cells using a dual electron transport layer of gold nanoparticles embedded in anatase TiO₂ films," ACS App. Energy Mat., vol. 3, pp. 9568–9575, 2020. http://dx.doi.org/10.1021/acsaem.0c00276.
- [4] M. B. Salim, R. Nekovei and A. Verma, "Modeling of plasmonic organic solar cells using core-shell metallic nanoparticles," 15th IEEE Int.Conference on Nano/Micro Eng. & Mole. Syst. (NEMS), vol. 1, pp. 422–425, 2020. https://doi.org/10.1109/NEMS50311.9265610.
- [5] M. Z. Toe, A. T. Le, S. S. Han, K. A. B. Yaacob and S. Y. Pung, "Silver nanoparticles coupled ZnO nanorods array prepared using photo-reduction method for localized surface plasmonic effect study," J. of Crys. Growth, vol. 547, 125806, 2020. https://doi.org/10.1016/j.jcrysgro.2020.125806.
- [6] B. Y. Tay, S. Y. Chee, C. L. Lee, S. Sepeai and M. Aminuzzaman, "Improvement of light-harvesting efficiency of amorphous silicon solar cell coated with silver nanoparticles anchored via (3-mercaptopropyl) trimethoxysilane," App. Nanosci., vol. 10, pp. 3553–3567, 2020. https://doi.org/10.1007/s13204-020-01478-9.
- [7] W. J. Ho, K. Y. Hsiao, C. H. Hu, T. W. Chuang, J. J. Liu and Y. H. Chen, "Characterized plasmonic effects of various metallic nanoparticles on silicon solar cells using the same anodic aluminum oxide mask for film deposition," Thin Solid Films, vol. 631 pp. 64–71, 2017. https://doi.org/10.1016/j.tsf.2017.04.016.
- [8] E. Jbira, H. Derouiche and K. Missaoui, "Enhancing effect of silver nanoparticles (AgNPs) interfacial thin layer on silicon nanowires (SiNWs)/PEDOT: PSS hybrid solar cell," Solar Energy, vol. 211, pp. 1230– 1238, 2020. https://doi.org/10.1016/j.solener.2020.09.090.

- [9] S. Sreeja and B. Pesala, "Plasmonic enhancement of betanin-lawsone co-sensitized solar cells via tailored bimodal size distribution of silver nanoparticles," Sci. Rep., vol. 10, 65236, 2020. https://doi.org/10.1038/s41598-020-65236-1.
- [10] H. Tan, R. Santbergen, A.H.M. Smets & M. Zeman, "Plasmonic light trapping in thin-film silicon solar cells with improved self-assembled silver nanoparticles," Nano Lett., vol. 12, pp. 4070–4076, 2012. https://doi.org/10.1021/nl301521z.
- [11]E. Danladi, M. Y. Onimisi, S. Garba, P. M. Gyuk, T. Jamila and H. P. Boduku, "Improved power conversion efficiency in perovskite solar cell using silver nanoparticles modified photoanode," IOP Conf. Series: Mat. Sci. & Eng., vol. 805, 012005, 2020. https://doi.org/10.1088/1757-899X/805/1/012005.
- [12]E. Danladi et al., "9.05 % HTM free perovskite solar cell with negligible hysteresis by introducing silver nanoparticles encapsulated with P4VP polymer," SN App. Sci., vol. 2, pp. 1769, 2020. https://doi.org/10.1007/s42452-020-03597-y.
- [13] C. Zhi, Z. Li and B. Wei, "Recent progress in stabilizing perovskite solar cells through two-dimensional modification," APL Mat., vol. 9, 070702, 2021. https://doi.org/10.1063/5.0056106.
- [14] L. P. Silva, I. Reis and C. C. Bonatto, "Green synthesis of metal nanoparticles by plants: current trends and challenges," Green Process Nanotech., vol. 9, pp. 327–352, 2015. https://doi.org/10.1007/978-3-319-15461-9 9.
- [15] A. K. Jha, A. K. J. Prasad, K. Prasad and A. R. Kulkarni, "Plant system: nature's nanofactory," Colloids and Surfaces B: Biointerfaces, vol. 73, pp. 219–223, 2009. https://doi.org/10.1016/j.colsurfb.2009.05.018.
- [16] Y. A. Akimov, W. S. Koh, S. Y. Sian and S. Ren, "Nanoparticles-enhanced thin film solar cells: Metallic or dielectric nanoparticles?," App. Phy. Lett., vol. 96, 073111, 2010. https://doi.org/10.1063/1.3315942.
- [17]T. V. Pfeiffer, J. Ortiz-Gonzalez, R. Santbergen, A.H.M. Smets and M. Zeman, "Plasmonic nanoparticle films for solar cell applications fabricated by size-selective aerosol deposition," Energy Procedia, vol. 60, pp. 3–12, 2014. https://doi.org/10.1016/j.egypro.2014.12.335.
- [18] J. Tasiu et al., "Dye sensitized solar cells with silver nanoparticles in nanocomposite photoanode for exploring solar energy concept," J. of Nanomat. Sci. Res., vol. 1, pp. 16–21, 2022. https://doi.org/10.20221/jnmsr.v1i.1.

- [19]E. Danladi, I. Andrew, D. O. Emmanuel, S. A. Damilare, E. O. Elijah, M. E. Ohi and O. A. Daniel, "Broad-band-enhanced and minimal hysteresis perovskite solar cells with interfacial coating of biogenic plasmonic light trapping silver nanoparticles," Mat. Res. Innov., 2023. https://doi.org/10.1080/14328917.2023.2204585.
- [20] Q. Luo, C. Zhang, X. Deng, H. Zhu, Z. Li, Z. Wang, X. Chen and S. Huang, "Plasmonic effects of metallic nanoparticles on enhancing performance of perovskite solar cells," ACS App. Mat. & Interfaces, vol. 9, pp. 34821–34832, 2017. https://doi.org/10.1021/acsami.7b08489.